UC Santa Barbara

UC Santa Barbara Previously Published Works

Title

An Optogenetic Platform to Dynamically Control the Stiffness of Collagen Hydrogels.

Permalink

https://escholarship.org/uc/item/3070r8kr

Journal

ACS biomaterials science & engineering, 7(2)

ISSN

2373-9878

Authors

Hopkins, Erik
Valois, Eric
Stull, Alanna
et al.

Publication Date

2021-02-01

DOI

10.1021/acsbiomaterials.0c01488

Peer reviewed

eScholarship.org Powered by the California Digital Library
University of California

Author Manuscript

Author Manuscript

Author Manuscript

Author Manuscript

HHS Public Access

Author manuscript

ACS Biomater Sci Eng. Author manuscript; available in PMC 2021 October 25.

Published in final edited form as:

ACS Biomater Sci Eng. 2021 February 08; 7(2): 408–414. doi:10.1021/acsbiomaterials.0c01488.

An Optogenetic Platform to Dynamically Control the Stiffness of Collagen Hydrogels

Erik Hopkins[*,1], **Eric Valois**[*,1,3,4], **Alanna Stull**[1], **Kristy Le**[1], **Angela A. Pitenis**[4], **Maxwell Z. Wilson**[1,2,3,†]

[1]Department of Molecular, Cellular, and Developmental Biology, University of California, Santa Barbara. Santa Barbara, CA 93106, United States

[2]Neuroscience Research Institute, University of California, Santa Barbara. Santa Barbara, CA 93106, United States

[3]Center for BioEngineering, University of California, Santa Barbara. Santa Barbara, CA 93106, United States

[4]Materials Department, University of California, Santa Barbara. Santa Barbara, CA 93106, United States

Abstract

The extracellular matrix (ECM) is comprised of a meshwork of biomacromolecules whose composition, architecture, and macroscopic properties, such as mechanics, instruct cell fate decisions during development and disease progression. Current methods implemented in mechanotransduction studies either fail to capture real-time mechanical dynamics or utilize synthetic polymers that lack the fibrillar nature of their natural counterparts. Here we present an optogenetic-inspired tool to construct light-responsive ECM mimetic hydrogels comprised exclusively of natural ECM proteins. Optogenetic tools offer seconds temporal resolution and submicron spatial resolution, permitting researchers to probe cell signaling dynamics with unprecedented precision. Here we demonstrated our approach of using SNAP-tag and its thiol-targeted substrate, benzylguanine-maleimide, to covalently attach blue-light responsive proteins to collagen hydrogels. The resulting material (OptoGel) –in addition to encompassing the native biological activity of collagen– stiffens upon exposure to blue light and softens in the dark. Optogels have immediate use in dissecting the cellular response to acute mechanical inputs and may also have applications in next-generation bio-interfacing prosthetics.

Graphical Abstract

[†]Corresponding author, mzw@ucsb.edu.
[*]These authors contributed equally to this work

SUPPORTING INFORMATION

Photoswitchability and BG-Mal binding of EL222-SNAP; Collagen alexa555-maleimide staining; OptoGel production schematic; HeLa cell viability data; Representative force-indentation curve; Pore size data; EL222-SNAP amino acid sequence; Sequential activation elastic moduli

Author Manuscript Author Manuscript Author Manuscript Author Manuscript

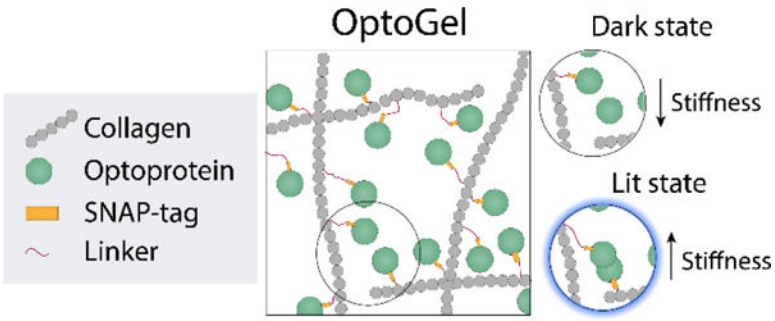

Keywords

Optogenetics; Dynamic ECM; Collagen Functionalization; “Click” Chemistry; ECM-mimetic Substrate

INTRODUCTION

Conventional hydrogels are passive scaffolds of synthetic or biological polymers largely utilized for their ability to interface with biological surfaces.[1] Their molecular architecture gives rise to macroscale properties, such as stiffness,[2] that determine their biological efficacy. Recently, there has been a growing appreciation for the importance of a surface’s mechanical properties in steering the decision-making networks of an enormous range of cells and organisms.[3–6] Thus, the ability to tune the macroscale properties of hydrogels is crucial for their application in tissue engineering, cell culture, pharmaceuticals, diagnostics, implants, and, even contact lenses.[7]

The combined sensing of mechanical and chemical cues driving cell fate decisions during development and initiating cellular dysfunction in disease necessitates an extracellular environment that can precisely mimic the dynamic cellular boundary conditions that cells experience *in vivo*. Stimuli-responsive hydrogels made from naturally occurring ECM proteins, in which a user-defined input alters the chemical or mechanical functionality of the gel, can provide this ability *in vitro*. Previously, hydrogels have been engineered to stiffen, soften, or release embedded molecules as a result of chemically- or photo- induced restructuring of the polymer network.[8–10] While such materials have unlocked the ability to acutely perturb the mechanical environment of cells, they either lack reversibility or are designed with synthetic polymers that form an amorphous, non-fibrillar, network. Thus, they fail to recapitulate the time-varying, chemically and structurally complex nature of the extracellular environment (ECM).[11–13]

The incorporation of photo-switchable proteins, whose binding state can be toggled with light, into synthetic hydrogel networks has resulted in bidirectionally dynamic materials.[14,15] Such hydrogels can cycle between material states in a light-dependent fashion, transmitting mechanical inputs to embedded cells. Recently, a synthetic polyethylene glycol (PEG) hydrogel functionalized with a red-light photo-switchable protein showed reversible mechanical activation.[14] While such materials allow the study of dynamic mechanical inputs to cells, PEG is biologically inert and requires the addition of cell-

Author Manuscript Author Manuscript Author Manuscript Author Manuscript

recognition motifs to support cell growth.[16] Although the chemical nature of PEG (and other synthetic gel-forming polymers) facilitates such modifications, a widespread movement toward more physiologically relevant culture platforms highlights the need for an easily-disseminatable method to control the mechanical properties of ECM mimetic substrates. Thus, to retain the biochemical and mechanical complexity of natural ECM, we sought to reversibly control the mechanical properties of a natural ECM-forming polymer.

Collagen Type I is a ubiquitous hydrogel-forming protein that plays a key role in shaping ECM mechanics and signaling in vertebrates.[17] Post-translational modifications and a fibrillar structure give rise to intrinsic signaling capabilities essential for proper cell function.[6,18–20] Despite its relevance, collagen's utility is limited by its finite functionalization chemistries and low-yield recombinant purification.[21] Animal-extracted collagen is easily attainable and commonly modified with crosslinking or mineralization agents to achieve hydrogels of desired stiffnesses,[3,22] however these mechanisms are unidirectional and tend to occupy cell recognition sites that diminish collagen's intrinsic bioactivity.[23]

Here we report a promising platform technology for creating reversible, stimuli-responsive ECM for any thiol containing biopolymer. The modular design consists of three constituent components. i) A translational fusion between a photo-switchable protein and SNAP-tag enzyme (Opto-SNAP),[24] ii) a thiol-containing biopolymer (Rat tail Collagen, Corning), and iii) a targeted heterofunctional SNAP-tag substrate (benzylguanine-maleimide) (Fig. 1A). We show that benzylguanine-maleimide (BG-Mal) covalently links Opto-SNAP proteins to a collagen hydrogel (OptoGel), offering an alternative to recombinant ECM modification. OptoGels dynamically mimic biologically relevant tissue stiffness changes, that can influence cell fate decisions in development and disease,[14,25] through blue light stimulation. The ease with which OptoGels are assembled and their ability to precisely mimic natural ECM may greatly facilitate cellular mechanical studies.

RESULTS

SNAP-tag Fusion Design

The core component of our OptoGels is a purified "optogenetic" protein that can occupy two self-association states, one with a substantially greater dissociation constant (K_d) than the other, depending on whether it has absorbed the energy from a photon of a particular wavelength of light.[26] To begin we chose to work with the Lov-domain containing protein EL222, a blue light– responsive protein from *Erythrobacter litoralis*.[27] EL222 undergoes a well-documented conformational rearrangement in the presence of blue light, whose switching efficiency peaks at 450nm light, to expose a high affinity homodimerization interface.[28] We hypothesized that covalently linking EL222 to gelled collagen by creating a SNAP-tag - EL222 fusion protein (EL222-SNAP) would permit light-programmable stiffening caused by the formation of nascent crosslinks resulting from the light-induced decrease in EL222-EL222 K_d, as the EL222 homodimers would act analogously to crosslinks (Fig. 1B).

Author Manuscript Author Manuscript Author Manuscript Author Manuscript

From the N- to C- terminus, EL222-SNAP consists of a 6x His tag to aid in purification, mCherry-FP to permit visualization of functionalized collagen hydrogels (OptoGel), a TEV cleavage site followed by EL222, a 6 amino acid GS linker, and the SNAP tag enzyme (Fig. 2A, Table S1). The TEV cleavage site is intended to allow removal of the fluorescent reporter and aids in construct identification. This construct, EL222-SNAP, was expressed and purified through E. coli bacterial expression, metal affinity chromatography, and size exclusion chromatography. Correct expression was verified via western blotting with anti-His and anti-SNAP-tag antibodies directed against the N- and C- termini, respectively. Colocalization of signal corresponding to anti-His and anti-SNAP-tag at 75 kDa indicated the presence of a full-length construct (Fig. 2B). Matrix Assisted Laser Desorption Ionization Time of Flight Mass Spectrometry (MALDI-TOF MS) of purified EL222-SNAP produced a m/z peak at 74.4 (Fig. 2C, *red*). An overnight TEV digestion of EL222-SNAP produced two distinct peaks at 30 and 44.2 (Fig. 2C, *blue*), corresponding to the N- and C- terminal products of EL222-SNAP and confirming the successful purification of our synthetic product. We noted the presence of minor degradation products from the full-length product in both western blots and MS (Fig. 2B,C), however these did not appear to influence EL222-SNAP function or subsequent experiments.

EL222-SNAP Functionality

Purified EL222-SNAP must be both light-responsive and efficiently conjugate BG-Mal in order to engineer reversible, light-tunable OptoGels. Thus, after purifying EL222-SNAP we sought to verify that it was fully functional. In the absence of blue light, EL222-SNAP exhibits an absorbance peak at 450 nm, consistent with published reports of EL222.[28] Upon illumination, this peak decreased (Fig 2E), indicating that our recombinant EL222-SNAP could indeed photo-actuate, consistent with Cys-FMN adduct formation and decreased K_d.[28] After removing blue light the 450 nm absorbance peak returned, indicating reversibility (Fig. S1A). Additionally, we tested EL222-SNAP's capacity to be cyclically photo switched and found no fatigue after 7 sequential activations (Fig. S1B). Finally, measurements of photoswitchability of purified EL222-SNAP over 20 days revealed no degradation in its ability to respond to light activation (Fig. S1E). Taken together these results demonstrate that the light-responsive functionality of EL222 is retained in the SNAP-tag fusion.

In order for EL222-SNAP dimerization to alter the OptoGel's stiffness it must be mechanically coupled through covalent attachment of the SNAP-tag domain to BG-Mal. To confirm this interaction, we compared MALDI-TOF mass spectrometry of EL222-SNAP with, and without, BG-Mal incubation. As expected, incubation with BG-Mal increased the mass of EL222-SNAP by 650 Da, consistent with the mass of BG-Mal (Fig. 2D). TEV protease digestion of EL222-SNAP, which cleaves the His-mCherry from EL222-SNAP, confirmed BG-Mal binds at the C-terminal SNAP-tag (Fig. S1C, S1D). Together, these results indicate that our purified EL222-SNAP has the functional characteristics required to engineer reversibly photo-switchable biopolymers.

Functionalization of Collagen Hydrogels with Opto-SNAP

After establishing the functionality of EL222-SNAP, we next sought to use this tool to functionalize off-the-shelf collagen hydrogels. Collagen is an ideal substrate to

Author Manuscript Author Manuscript Author Manuscript Author Manuscript

demonstrate this platform due to its ease of handling, ubiquitous use in cell culture and bioengineering,[11,29,30] and high mole ratio of cysteine residues (~17/molecule). This final attribute permits a high degree of functionalization via thiol-maleimide click chemistry between BG-Mal and collagen-residing cysteine residues.

The presence of solvent-accessible cysteine residues in collagen hydrogels was first assessed with Alexa555-maleimide. The strong fluorescent signal seen in Alexa555 modified hydrogels, even after multiple washes, indicated extensive availability of modification sites (Fig. S2A). By utilizing BG-Mal as a directionally specific linker for SNAP-tag and thiols, a variety of Opto-SNAP fusion proteins can be tethered to the collagen network with equivalent maleimide-thiol click chemistry. We tested different BG-Mal concentrations to determine the most effective approach for attaching Opto-SNAPs. 100μM was the only concentration resulting in a stiffness increase after completing functionalization and activation. Therefore we used 100 μM BG-Mal for all subsequent experiments (Fig. S2B). To avoid BG-Mal reacting with surface-exposed thiols on EL222, which could conjugate EL222-SNAP monomers and compromise their function, collagen hydrogels were incubated with BG-Mal prior to the addition of EL222-SNAP, resulting in specific, covalent coupling of EL222-SNAP to collagen (Fig. S3). The resulting hydrogels showed mCherry fluorescence with clearly discernable collagen fibrils (Fig. 3A, *right*). Hydrogels incubated with EL222-SNAP but lacking BG-Mal, resulted in the absence of fluorescent fibrils (Fig. 3A, *left*) demonstrating that EL222-SNAP coupling to collagen is BG-Mal dependent.

To establish OptoGels as a useful tool for cell mechanics studies they must support cell growth in a similar manner to commonly used surfaces, such as collagen and glass. We confirmed that HeLa cells plated on EL222 OptoGels maintained a similar viability and metabolism to cells on collagen and glass substrates over a 7-day period, thus confirming that the EL222-SNAP functionalization is non-toxic (Fig. S4).

Light Dependent Mechanics of OptoGels

As discussed previously, EL222 undergoes a structural rearrangement when activated to expose a high-affinity dimerization site.[28] Notably, the relationship between crosslink density of collagen and resulting stiffness is well documented, and even exploited evolutionarily to yield tissues of varying mechanical properties.[2,31] Thus, we hypothesized that EL222-SNAP dimerization within OptoGels would act as reversible crosslinks, therefore stiffening the OptoGel in the presence of light. To discern the stiffness dynamic range achievable with EL222 OptoGels we subject them to blue light illumination while simultaneously measuring stiffness using IT-AFM. We found a statistically significant 22% increase in elastic modulus of EL222 OptoGels (196 Pa to 239 Pa) (n = 9) (Fig. 3B, Fig. S5). To accurately mimic the mechanically dynamic environment experienced by cells *in vivo*, OptoGels must reversibly soften and stiffen in response to activating light. To test if OptoGels can be reversibly toggled, we subject them to two rounds of sequential activation (10 min OFF, 10 min ON). The elastic moduli of the OptoGel after illumination was roughly 20% higher than that of the preceding dark state, thus confirming that OptoGels can undergo dynamic stiffening (Fig. 3C). To test if additional washes with purified EL222-SNAP increased the dynamic range we tested the mechanical toggling in a gel that had

Author Manuscript Author Manuscript Author Manuscript Author Manuscript

been washed 2 additional times in EL222-SNAP for a total of 3 washes. While we found that these 3X OptoGels were an order of magnitude stiffer in their baseline dark state, upon activation they again stiffened to roughly 20% greater than their baseline (Fig. 3D, Absolute values reported in Table S2). Interestingly, dark-state stiffnesses decreased with each successive activation in both OptoGels, most likely as a result of gel fatigue.

A well-established relationship between substrate stiffness and pore size has been gleaned from experiments conducted on static hydrogels. Typically, pore size can be tuned by altering polymer concentration or polymerization.[32,33] Therefore, to interrogate the mechanism of stiffening in activated EL222 OptoGels, the pore size of an EL222 OptoGel was measured with confocal microscopy pre- and post-activation. In the basal state (i.e. no illumination), the average pore area was measured to be 1.6 μm^2 (Fig. S6). Despite blue light activation, our visual quantification revealed no change in pore size, however this method is limited to measuring changes of greater than the resolution limit of our optical system.

DISCUSSION

The mechanical and biochemical importance of the ECM is well established and continues to be an area of intense research. Until recently, the inability to dynamically control the mechanical properties of protein-based hydrogels has forced these two parameters to be studied either independently or in a static fashion, thus inadequately recapitulating the dynamics of the extracellular environment.[34] As the most abundant protein in the ECM, collagen is an obvious choice for creating *de novo* ECM mimetic materials. Collagen's hierarchical structure provides many unique opportunities for tuning macroscopic mechanical properties.[11,29] Parameters such as fiber dimensions, polymerization condition, and fibrillar crosslink density can be manipulated prior to polymerization, yielding hydrogels with variable, but static mechanical properties.[2,31,32] Considering these physical attributes are essential for many cell-scaffold interactions and mechanotransduction.[13,18–20] the field is limited to varying the properties of static gels and extrapolating between conditions to predict how cells would respond to *in vivo*. While this approach has uncovered several relationships between substrate mechanics and cell fate decisions, it fails to capture real time changes that occur during development and disease.[3,4,6,35]

Our solution leverages the combined attributes from light responsive proteins and the SNAP-tag enzyme. The resulting fusion protein has several key advantages for engineering ECM mimetic hydrogels. First, opto-proteins photo-switch within milliseconds of stimuli application,[36] allowing the ability to reversibly toggle material changes within physiologically relevant timeframes. Second, BG-Mal click chemistry makes for facile modification of most proteins via peptidyl thiols. Other commercially available benzylguanine derivates are designed to target carboxyl- or amine- functional groups, thus offering the possibility to engineer heterofunctionalized proteins and non-protein-based ECM components, such as hyaluronic acid. In comparison to classical collagen crosslinking methods such as 1-ethyl-3-(3-dimthyllamino-propyl)carbodiimide (EDC), thiol-maleimide click chemistry avoids compromising nucleophilic amines necessary for robust cell-substrate interactions.[37] While the work presented here demonstrates the effects of homo-dimerization upon illumination, other classes of opto-proteins exist, including homo-

Author Manuscript Author Manuscript Author Manuscript Author Manuscript

and hetero-oligomerizers and dark-inducible protein complexes, offering a suite of options for engineering dynamic stimuli-responsive materials.[38–40]

By conjugating EL222 to Collagen Type 1 we were able to create a collagen hydrogel with programmable mechanical properties. While the first iteration of our OptoGels demonstrated a modest dynamic range (~22%) in comparison to other optoprotein-based dynamic substrates, who stiffen on the order of kilopascals,[14] such stiffness increases have been shown to increase integrin expression and drive invasion of mammary epithelial cells.[25] In future work we plan to increase the dynamic range of OptoGels by engineering Opto-SNAPs with increased oligomerization states (oligomeric vs. dimeric), however the aforementioned studies highlight potential immediate uses for OptoGels. Importantly, EL222 OptoGels underwent two rounds of reversible stiffening, highlighting their use in modeling complex mechanical dynamics. As previously mentioned, the relationship between mesh size and material stiffness has been well documented. Thus, we anticipated mesh network contraction during stimulation. Contrary to our prediction, increased stiffness appeared independent of mesh size. We interpreted this result to mean that EL222-SNAP was forming nascent crosslinks between adjacent collagen fibrils, leading to increased crosslink density within the gel. Previous studies have shown such processes manifest increased stiffness independent of changes in pore size.[37,41,42] Future work may involve a combination of multiple crosslinking methods to first tune OptoGels to a desired baseline stiffness,[3,41] followed by functionalization to achieve dynamic control.

In summary, we describe an approach to create reversibly stiffening thiol-containing, biopolymer hydrogels using SNAP-tag coupling. As a proof of concept, we implemented this platform by coupling EL222-SNAP with Type 1 Collagen. We show that EL222-SNAP covalently binds collagen hydrogels in a BG-Mal dependent fashion and that the resulting hydrogel undergoes reversible increases in stiffness in a light-dependent fashion. Importantly, this technology combines collagen's intrinsic biological activity with the ability to tune mechanical properties, thus offering a user-regulated ECM-mimetic environment.

OptoGels provide an immediate opportunity to control acute mechanical cellular environments. Furthermore, by combining the existing OptoGel platform with advanced light delivery devices we hope to increase our control over the spatial and temporal dimensions. Additionally, by altering the 'Opto' module of Opto-SNAP to include light inducible release of signaling proteins, we plan to expand the capabilities of OptoGels to include control of chemical cellular environments. Thus, OptoGels may serve as a singular material capable of recapitulating the mechanical and biochemical components of native ECM.

MATERIALS AND METHODS

Synthesis and Purification of Opto-SNAP Constructs:

The EL222-SNAP expression plasmid was synthesized from the pBAD expression vector (Invitrogen), mCherry, peblindv2 (encoding residues 1–225 of EL222), and pSNAP-tag(T7) (NEB) using Gibson Assembly. Plasmids were transformed into *E. coli* TOP10 (Thermo Fisher Scientific) and transformed clones were selected by 100 μg/mL ampicillin. To express

Author Manuscript Author Manuscript Author Manuscript Author Manuscript

EL222-SNAP, an overnight culture was used to inoculate 1 liter of Terrific Broth (TB, IBI Scientific), supplemented with100 μg/mL ampicillin such that the OD600 was 0.01. The culture was grown at 37°C until the OD600 reached 0.4–0.6 at which point flasks were covered to keep the culture dark and 0.4% (w/v) arabinose was added to induce expression. *All steps after arabinose induction were carried out in the dark or under red light to prevent activation of EL222-SNAP.* After incubation at 25°C for 14–16 hour, bacteria were harvested by centrifugation, washed with 30mL PBS, and shock frozen in liquid nitrogen for future purification. To purify the EL222-SNAP, frozen pellets underwent 2 freeze/thaw cycles, and were resuspended in lysis buffer (20mM imidazole, 20mM Tris, 150mM NaCl, pH 8.0) supplemented with 0.25 mg/mL lysozyme (Sigma, 6867–1G) and 1% (v/v) Protease Inhibitor Cocktail (Sigma, P8849–5ML). After a 30 minute incubation at room temperature with gentle shaking, the solution was sonicated at 30% power with an ON:OFF cycle of 15 seconds : 45 seconds for a total time of 5 minutes. Cell lysates were clarified via centrifugation at 10,000g for 15 min. Clarified lysate was loaded onto a HiTrap High Performance Ni-NTA column (GE Healthcare) and separated using a BioRad NGC chromatography system (Bio-Rad Laboratories, Hercules CA). After sample loading, the column was washed with 5 column volumes of binding buffer (20 mM imidazole, 20mM Tris and 150mM NaCl pH 8.0) to remove unbound proteins. Proteins of interest were eluted from the column using binding buffer supplemented with imidazole (250 mM imidazole, 20mM Tris and 150mM NaCl pH 8) and quickly dialyzed to remove imidazole (20mM Tris and 150mM NaCl, pH 8.0). EL222-SNAP eluted from the His-Trap was further separated from unwanted proteins using a Superdex 75 10/300 GL size exclusion column. 500 μL of His-Trap elutant in dialysis buffer was loaded and separated using a flow rate of 400 μL/min while collecting 750μL fractions. Protein concentration and purity were determined with ultraviolet absorption (λ = 280 nm, Extinction Coefficient 75540 $M^{-1}cm^{-1}$ [Expasy protparam]) prior to aliquoting and freezing at −80°C for future use.

Light Responsiveness of Purified EL222-SNAP:

Purified EL222-SNAP was diluted to 0.5 mg/mL and subject to 1-minute blue light OFF-ON cycles (7x). Absorbance spectra from 200 nm to 900 nm was measured at 5 second increments with an IMPLEN NP80 spectrophotometer. Blue light was delivered by a single 450nm LED powered with a 9V battery placed over the sample.

TEV Cleavage:

Purified EL222-SNAP was diluted to 1 mg/mL and incubated with 1 μL TEV (2 mg/mL) (Sigma) in a 250 μL reaction. The sample was protected from light and digested overnight at room temperature. Cleaved samples were used for further characterization via Mass Spectrometry, incubation with BG-Maleimide (NEB, S9153S), or loaded onto a HiTrap High Performance Ni-NTA column (GE Healthcare) for separation. For samples loaded into the affinity column, both the wash (Buffer A) and elutant (Buffer B) were saved, dialyzed into Buffer C, and examined with western blot analysis using anti-His (SC Biotech, SC-53073) and anti-SNAP (NEB, P9310S) antibodies.

Additional samples, both TEV-treated and -untreated, were incubated with 100 μM BG-Maleimide (NEB, S9153S) overnight at room temperature, and dialyzed into buffer C

Author Manuscript Author Manuscript Author Manuscript Author Manuscript

to remove excess BG-Maleimide. Dialyzed samples were used for characterization with MALDI-TOF Mass Spectrometry.

OptoGel Handling and Preparation:

To promote adhesion of collagen to glass surfaces for subsequent mechanical and cellular tests, surfaces were treated with silanol followed by glutaraldehyde. Briefly, 15mm glass cover slips (#1.5) were cleaned in a bath of ethanol for 24 hours and then dried in the oven at 155°C for 1 hour. Clean surfaces were in incubated in excess 2% 3-Aminopropyl)triethoxysilane (Sigma-Aldrich) in ethanol for 1 hours at room temperature will orbital shaking at 30rpm. Surfaces were then rinsed with excess ethanol and heated at 37°C overnight. Silanted surfaces were subsequently treated with 2% glutaraldehyde (Electron Microscopy Sciences, # 16216–10) in PBS for 2hours at room temp. Surfaces were then rinsed with excess PBS (2X) and deionized water (2X) to remove excess glutaraldehyde and salt and dried using a sterile air stream before being used to support hydrogels.

Collagen hydrogels were synthesized from rat-tail collagen (Corning, 354249) per the manufacturer's suggestion. Briefly, 1 mg/mL hydrogels (70 μL) were prepped from a high-concentration collagen stock (9.4 mg/mL), 1M NaOH, 10x PBS and water. Hydrogel solution was incubated at 37°C for 45 minutes to induce gelation. After gelation, hydrogels to be imaged with Alexa555-maleimide (Thermo) were incubated in 100 nM dye solution for 2 hours at room temperature. Hydrogels were washed 3 times with PBS to remove unbound dye and stored at 4°C until imaging.

Hydrogels to be functionalized to OptoGels were incubated in 100 μM BG-maleimide for 1 hour at room temperature. Unbound BG-Mal was removed with 3x PBS washes. Hydrogels were further incubated in 4.5 mg/mL EL222-SNAP overnight at room temperature and washed the following day. *All opto protein incubations and proceeding steps were done in the dark to prevent aberrant opto-protein activation*. Hydrogels were stored submerged in the dark in PBS at 4°C until experiments.

HeLa cell culture and viability assays:

HeLa cells were stored at 37°C and 5% CO in T25 flasks in Dulbecco's Modified Eagle Medium (DMEM) containing 10% fetal bovine serum and 1% antibiotic (25units/mL penicillin, 25μg/mL streptomycin)(Invitrogen). For alamarBlue and Live/Dead assays, 96-well glass bottom dishes (Cellvis, Mountain View, CA) were salinated as previously described and 50μL collagen hydrogels were cast in the bottom of the wells and functionalized with EL222-SNAP. Cells were plated at a density of 10,000 cells/well in and monitored over 7 days. Metabolic activity was visualized using media supplemented with 10% alamarBlue solution following manufacturers protocol. 100uL samples of media were taken after a 1 hour incubation at 37°C and fluorescence signal (Ex/Em 560nm/590nm) was read with a plate reader (Biotek). After incubation in alamarBlue-supplemented media, cells were washed with PBS, DMEM, and replenished with fresh media.

Live versus dead cells were quantified using a LIVE/DEAD Viability/Cytotoxicity Kit (Thermo). Cells were washed once with PBS and incubated in 2μM Calcein-AM and 4

Author Manuscript Author Manuscript Author Manuscript Author Manuscript

μM ethidium homodimer-1 for 45 minutes at 37°C prior to imaging. Images were captured on a Nikon Super Resolution Spinning Disk Confocal microscope and live/dead cells were identified by custom FIJI macros or by hand, depending on cell density.

Pore Size Determination:

EL222 OptoGels were visualized with a spinning disk super resolution confocal microscope (Nikon) with a 60X water-immersion lens and 1.5X multiplier. Gels were activated with 1 second pulses of 100% 447 nm laser every 5 seconds for 10 minutes. mCherry on EL222-SNAP was utilized to visualize the microarchitecture of OptoGels. The hydrogel was visualized as 5 μM Z-stacks with slices every 0.3 μM (18 slices in total). Slices were taken with the following settings: 100% 561 nm laser, 100 ms exposure, sum of 8 images. Images used for pore size determination were constructed from 3 adjacent slices combined as average intensity projections. 4 different 40 μM x 40 μM areas, before and after activation, were analyzed in FIJI using elliptical ROIs to identify pores. Images were randomized, to prevent biased between pre- and post- activation and subject to analysis by three individuals.

IT-AFM:

Images and force measurements were conducted on a MFP-3D Bio (Asylum Research, Santa Barbara, CA). SICON-TL-SiO_2-A silicon tips with a 5μm radius probe (APPNano, Mountain View, CA) were used in all experiments. Gels were cast onto 10mm mica discs (TedPella, Inc) glued to standard microscope slides. All experiments were conducted within 24 hours of casting. Samples are loaded into the AFM scanning stage and subsequently submerged in PBS. Submerged samples were allowed to equilibrate in the instrument for 30min. Prior to force measurements, the cantilever spring constant was experimentally determined by the thermal tune method usually ranging between 0.5 to 1 N/m. Deflection sensitivity was calculated using a glass slide as an indefinitely stiff calibrant material. Force spectroscopy measurements were conducted over the maximum piezo travel length at 2 μm/s load/unload rate with a maximal loading force of 20 nN. Stiffness and values were calculated by Asylum Research's Elastic Analysis Tool by fitting the lower 10% of the loading curve, a probe radius of 5000 nm and a Poisson ratio of 0.5 to the Hertz Model.

MALDI-TOF Mass Spectrometry:

EL222-SNAP identity was assessed using MALDI-TOF MS. Purified protein diluted to 1 mg/mL was mixed 1:10 with MALDI-matrix, a saturated solution of Sinapinic acid in 50% Acetonitrile 1% trifluoroacetic acid. The protein solution was then applied to a 96 spot MALDI target plate (Bruker) and air dried for 30 min. Mass spec analysis was conducted using a Microflex LRF MALDI-TOF (Bruker). Sample targets were irradiated using a Nitrogen laser at 337 nm and a pulse length of 3ns with a repetition rate of 20 Hz. Detection occurred in linear mode between 20–80kDa at sampling rate of 1 Gs/s. Protein Calibration Standard 1 (Bruker #206355) was used as an internal calibration.

Sample Illumination:

Photoswitching and AFM samples from experiments detailed in main text figures 2 and 3 and supplementary figures 1, 2, 5, and 6 were illuminated at a distance of 4 cm from the

Author Manuscript Author Manuscript Author Manuscript Author Manuscript

sample using a home-built blue LED resulting in a surface power density of approximately 10 mW/cm^2 at 450nm. Light power was measured using a ThorLabs S121C photodiode power sensor with a 500mW max rating.

Statistical Analysis:

All scatter plots are presented as mean + Standard Deviation. Student t-tests were performed on all data sets using the MatLab function *ttest2* with significance of $P<0.05$ denoted by *.

Supplementary Material

Refer to Web version on PubMed Central for supplementary material.

ACKNOWLEDGEMENTS

The authors acknowledge support from the California Nanosystems Institute (CNSI), supported by the University of California, Santa Barbara and the University of California, Office of the President. E.V. and A.A.P. were supported by the MRSEC Program of the National Science Foundation under Award No. DMR 1720256.

REFERENCES

1. Peppas NA, Hilt JZ, Khademhosseini A & Langer R Hydrogels in Biology and Medicine: From Molecular Principles to Bionanotechnology. Adv. Mater 18, 1345–1360 (2006).
2. Lin S, Gu L, Editor A & Zadpoor AA Influence of Crosslink Density and Stiffness on Mechanical Properties of Type I Collagen Gel. Materials (Basel) 8, 551–560 (2015). [PubMed: 28787956]
3. Caprio N. Di & Bellas E Collagen Stiffness and Architecture Regulate Fibrotic Gene Expression in Engineered Adipose Tissue. Advacned Biosyst 4, (2020).
4. Ri Seo B, Chen X, Ling L, Hye Song Y, Shimpi AA, Choi S, Gonzalez J, Sapudom J, Wang K, Andresen Eguiluz RC, Gourdon D, Shenoy VB & Fischbach C Collagen microarchitecture mechanically controls myofibroblast differentiation. Proc. Natl. Acad. Sci (2020).
5. Siryaporn A, Kuchma SL, O'toole GA & Gitai Z Surface attachment induces Pseudomonas aeruginosa virulence. Proc. Natl. Acad. Sci 111, 16860–16865 (2014). [PubMed: 25385640]
6. Kawahara K, Yoshida T, Maruno T, Oki H, Ohkubo T, Koide T & Kobayashi Y Spatiotemporal regulation of PEDF signaling by type I collagen remodeling. Proc. Natl. Acad. Sci (2020).
7. Laftah WA, Hashim S & Ibrahim AN Polymer Hydrogels: A Review. Polym. Plast. Technol. Eng 50, 1475–1486 (2011).
8. Stowers RS, Allen SC & Suggs LJ Dynamic phototuning of 3D hydrogel stiffness. PNAS 112, 1953–1958 (2015). [PubMed: 25646417]
9. Wang R, Yang Z, Luo J, Hsing I-M & Sun FB 12-dependent photoresponsive protein hydrogels for controlled stem cell/protein release. PNAS 114, 5912–5917 (2017). [PubMed: 28533376]
10. Yang Z, Yang Y, Wang M, Wang T, Francis Fok HK, Jiang B, Xiao W, Kou S, Guo Y, Yan Y, Deng X, Zhang W & Sun F Dynamically Tunable, Macroscopic Molecular Networks Enabled by Cellular Synthesis of 4-Arm Star-like Proteins. Matter 2, 233–249 (2020).
11. Caliari SR & Burdick JA A practical guide to hydrogels for cell culture. Nature Methods 13, 405–414 (2016). [PubMed: 27123816]
12. Hu W, Li Q, Li B, Ma K, Zhang C & Fu X Optogenetics sheds new light on tissue engineering and regenerative medicine. Biomaterials 227, 119546 (2020). [PubMed: 31655444]
13. Prince E & Kumacheva E Design and applications of man-made biomimetic fibrillar hydrogels. Nat. Rev. Mater 4, 99–115 (2019).
14. Hörner M, Raute K, Hummel B, Madl J, Creusen G, Thomas OS, Christen EH, Hotz N, Gübeli RJ, Engesser R, Rebmann B, Lauer J, Rolauffs B, Timmer J, Schamel WWA, Pruszak J, Römer W, Zurbriggen MD, Friedrich C, Walther A, Minguet S, Sawarker R & Weber W Phytochrome-Based Extracellular Matrix with Reversibly Tunable Mechanical Properties. Adv. Mater 1806727 (2019).

Author Manuscript Author Manuscript Author Manuscript Author Manuscript

15. Liu L, Shadish JA, Arakawa CK, Shi K, Davis J & DeForest CA Cyclic Stiffness Modulation of Cell-Laden Protein-Polymer Hydrogels in Response to User-Specified Stimuli Including Light Dynamic Biomaterials. Dyn. Biomater 2, 1800240 (2018).
16. Kyburz KA & Anseth KS Synthetic Mimics of the Extracellular Matrix: How Simple is Complex Enough? HHS Public Access Author manuscript. Ann Biomed Eng 43, 489–500 (2015). [PubMed: 25753017]
17. Yamauchi M & Sricholpech M Lysine post-translational modifications of collagen. Essays Biochem 52, 113–133 (2012). [PubMed: 22708567]
18. Baker BM, Trappmann B, Wang WY, Sakar MS, Kim IL, Shenoy VB, Burkick JA & Chen CS Cell-mediated fibre recruitment drives extracellular matrix mechanosensing in engineered fibrillar microenvironments. Nat. Mater 14, 1262–1270 (2015). [PubMed: 26461445]
19. Hynes RO The extracellular matrix: Not just pretty fibrils. Science 326, 1216–1219 (2009). [PubMed: 19965464]
20. Lou J, Stowers R, Nam S, Xia Y & Chaudhuri O Stress relaxing hyaluronic acid-collagen hydrogels promote cell spreading, fiber remodeling, and focal adhesion formation in 3D cell culture. Biomaterials 154, 213–222 (2018). [PubMed: 29132046]
21. Ruggiero F & Koch M Making recombinant extracellular matrix proteins. Methods 45, 75–85 (2008). [PubMed: 18442707]
22. Roether Id J, Bertels S, Oelschlaeger C, Bastmeyer M & Willenbacher N Microstructure, local viscoelasticity and cell culture suitability of 3D hybrid HA/collagen scaffolds. PLoS One (2018).
23. Grover CN, Farndale RW, Best SM & Cameron RE The interplay between physical and chemical properties of protein films affects their bioactivity. J. Biomed. Mater. Res. Part A 100 A, n/a-n/a (2012).
24. Jullerat, Gronmeyer, Keppler, Gendreizig, Pick, Vogel J Directed Evolution of O 6-Alkylguanine-DNA Alkyltransferase for Efficient Labeling of Fusion Proteins with Small Molecules In Vivo. Chem. Biol 10, 313–317 (2003). [PubMed: 12725859]
25. Levental KR, Yu H, Kass L, Lakins JN, Egeblad M, Erler JT, Fong SFT, Csiszar K, Giaccia A, Weninger W, Yamauchi M, Gasser DL & Weaver VM Matrix Crosslinking Forces Tumor Progression by Enhancing Integrin Signaling. Cell 139, 891–906 (2009). [PubMed: 19931152]
26. Takakado A, Nakasone Y & Terazima M Photoinduced dimerization of a photosensory DNA-binding protein EL222 and its LOV domain †. Phys. Chem. Chem. Phys 19, 24855 (2017). [PubMed: 28868541]
27. Zoltowski BD, Motta-Mena LB & Gardner KH Blue Light-Induced Dimerization of a Bacterial LOV−HTH DNA-Binding Protein. Biochemistry 52, 12 (2013).
28. Nash AI, McNulty R, Shilito ME, Swartz TE, Bogomolni RA, Luecke H & Gardner KH Structural basis of photosensitivity in a bacterial light-oxygen-voltage/helix-turn-helix (LOV-HTH) DNA-binding protein. Proc. Natl. Acad. Sci 108, 9499–9454 (2011).
29. Meyer M Processing of collagen based biomaterials and the resulting materials properties. Biomed. Eng. Online 18, (2019).
30. Marques CF, Diogo GS, Pina S, Oliveira JM, Silva TH & Reis RL Collagen-based bioinks for hard tissue engineering applications: a comprehensive review. Journal of Materials Science: Materials in Medicine 30, 1–12 (2019).
31. Depalle B, Qin Z, Shefelbine SJ & Buehler MJ Influence of cross-link structure, density and mechanical properties in the mesoscale deformation mechanisms of collagen fibrils. J. Mech. Behav. Biomed. Mater 52, 1–13 (2015). [PubMed: 25153614]
32. Yang Y-L, Leone LM & Kaufman LJ Elastic Moduli of Collagen Gels Can Be Predicted from Two-Dimensional Confocal Microscopy. Biophysj 97, 2051–2060
33. Taufalele PV, VanderBurgh JA, Muñoz A, Zanotelli MR & Reinhart-KingID CA Fiber alignment drives changes in architectural and mechanical features in collagen matrices. PLoS One (2019).
34. Geckil H, Xu F, Zhang X, Moon S & Demirci U Engineering hydrogels as extracellular matrix mimics. Nanomedicine 5, 469–484 (2010). [PubMed: 20394538]
35. Zhou Q, Lyu S, Bertrand AA, Hu AC, Chan CH, Ren X, Dewey MJ, Tiffany AS, Harley BAC & Lee JC Stiffness of Nanoparticulate Mineralized Collagen Scaffolds Triggers Osteogenesis via Mechanotransduction and Canonical Wnt Signaling. bioRxiv (2020).

Author Manuscript Author Manuscript Author Manuscript Author Manuscript

36. Iuliano JN, Gil AA, Laptenok SP, Hall CR, Tolentino Collado J, Lukacs A, Hag Ahmed SA, Abyad J, Daryee T, Greetham GM, Sazanovich IV, Illarionov B, Bachr A, Fischer M, Towrie M, French JB, Meech SR & Tonge PJ Variation in LOV Photoreceptor Activation Dynamics Probed by Time-Resolved Infrared Spectroscopy. Biochemistry 57, 620–630 (2018). [PubMed: 29239168]

37. Roeder BA, Kokini K, Sturgis JE, Robinson JP & Voytik-Harbin SL Tensile Mechanical Properties of Three-Dimensional Type I Collagen Extracellular Matrices With Varied Microstructure. J. Biomech. Eng 124, (2002).

38. Lungu OI, Hallett RA, Jung Choi E, Aiken MJ, Hahn KM & Kuhlman B Designing Photoswitchable Peptides Using the AsLOV2 Domain. Chem. Biol 19, 507–517 (2012). [PubMed: 22520757]

39. Zhou XX, Chung HK, Lam AJ & Lin MZ Optical control of protein activity by fluorescent protein domains. Science (80-.) 338, 810–814 (2012).

40. Taslimi A, Vrana JD, Chen D, Borinskaya S, Mayer BJ, Kennedy MJ & Tucker CL An optimized optogenetic clustering tool for probing protein interaction and function. Nat. Commun (2014).

41. Davidenko N, Schuster CF, Bax DV, Raynal N, Farndale RW, Best SM & Cameron RE Control of crosslinking for tailoring collagen-based scaffolds stability and mechanics. Acta Biomater 25, 131–142 (2015). [PubMed: 26213371]

42. Greenfield MA, Hoffman JR, Olvera De La Cruz M & Stupp SI Tunable Mechanics of Peptide Nanofiber Gels. Langmuir 26, 3641–3647 (2010). [PubMed: 19817454]

Author Manuscript Author Manuscript Author Manuscript Author Manuscript

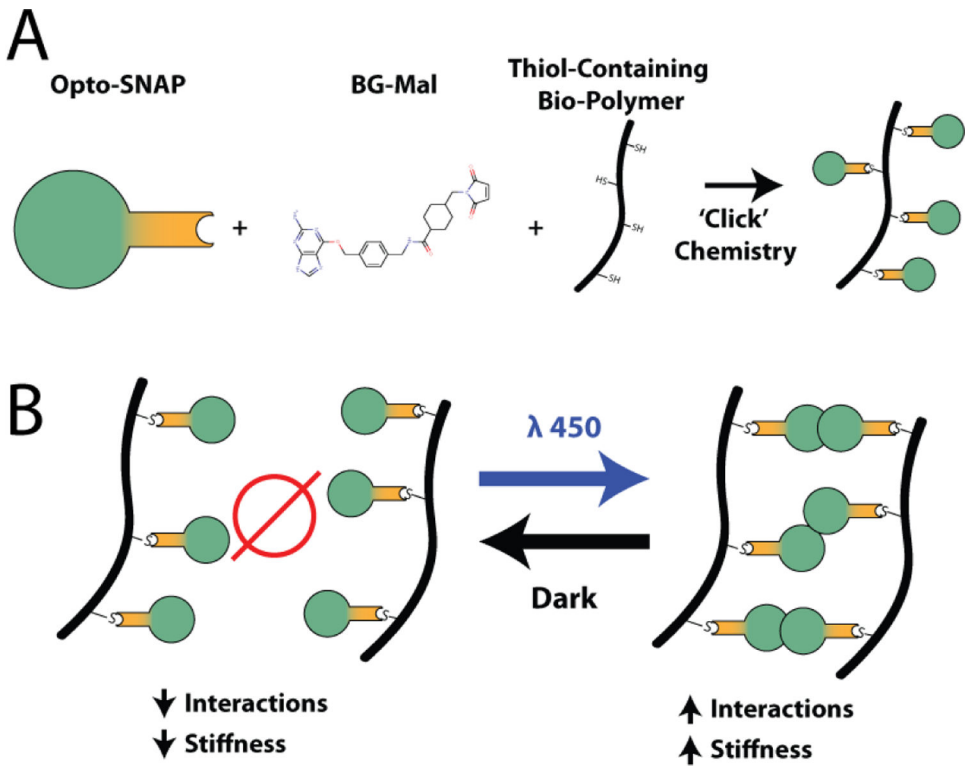

Figure 1. Polymer Functionalization Platform.

A) Three-piece functionalization platform consisting of a SNAP-tag fusion protein (Opto-SNAP), benzylguanine maleimide, and a cysteine-containing polymer. B) Activation of Optoprotein-SNAP-tag fusion proteins, when attached to polymers through the aforementioned system, increases polymer-polymer interactions, thus stiffening the gel.

Author Manuscript Author Manuscript Author Manuscript Author Manuscript

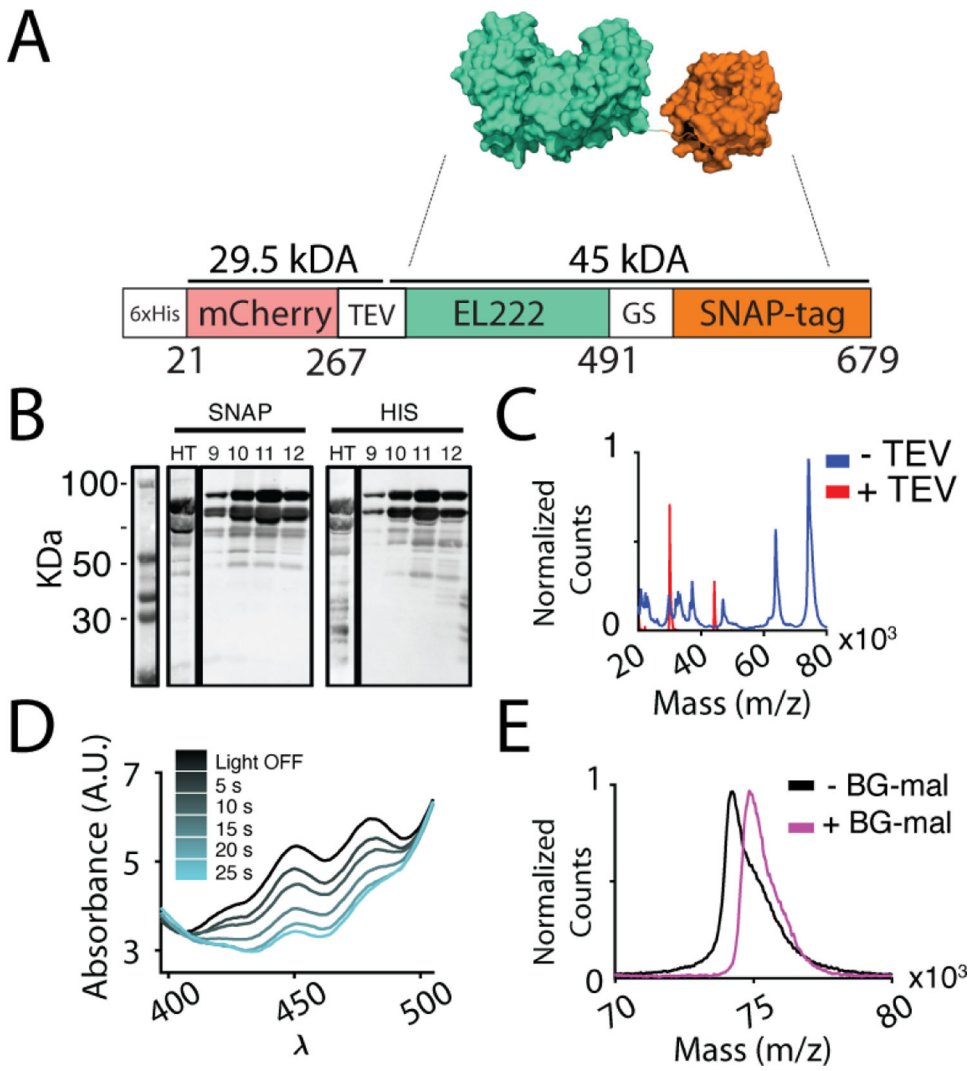

Figure 2. EL222-SNAP Retains Photoswitchability and BG-Mal Reactivity.

A) EL222-SNAP fusion consisting of purification tag, mCherry, EL222, a GS linker, and SNAP-tag. B) Western Blot analysis of purified EL222-SNAP (HT) and collected SEC fractions (9–12) with anti-SNAP (*left*) and anti-His (*right*) antibodies confirm the presence of a C-terminal SNAP-tag and N-terminal His-tag, respectively. C) MALDI-TOF mass spectrometry of full-length EL222-SNAP (*blue*) and TEV-digested EL222-SNAP (*red*). D) Decrease in absorbance at 450 nm of EL222-SNAP during 25 seconds of blue light activation. E) Mass increase of ~650 Da of EL222-SNAP when incubated with BG-Mal.

Author Manuscript Author Manuscript Author Manuscript Author Manuscript

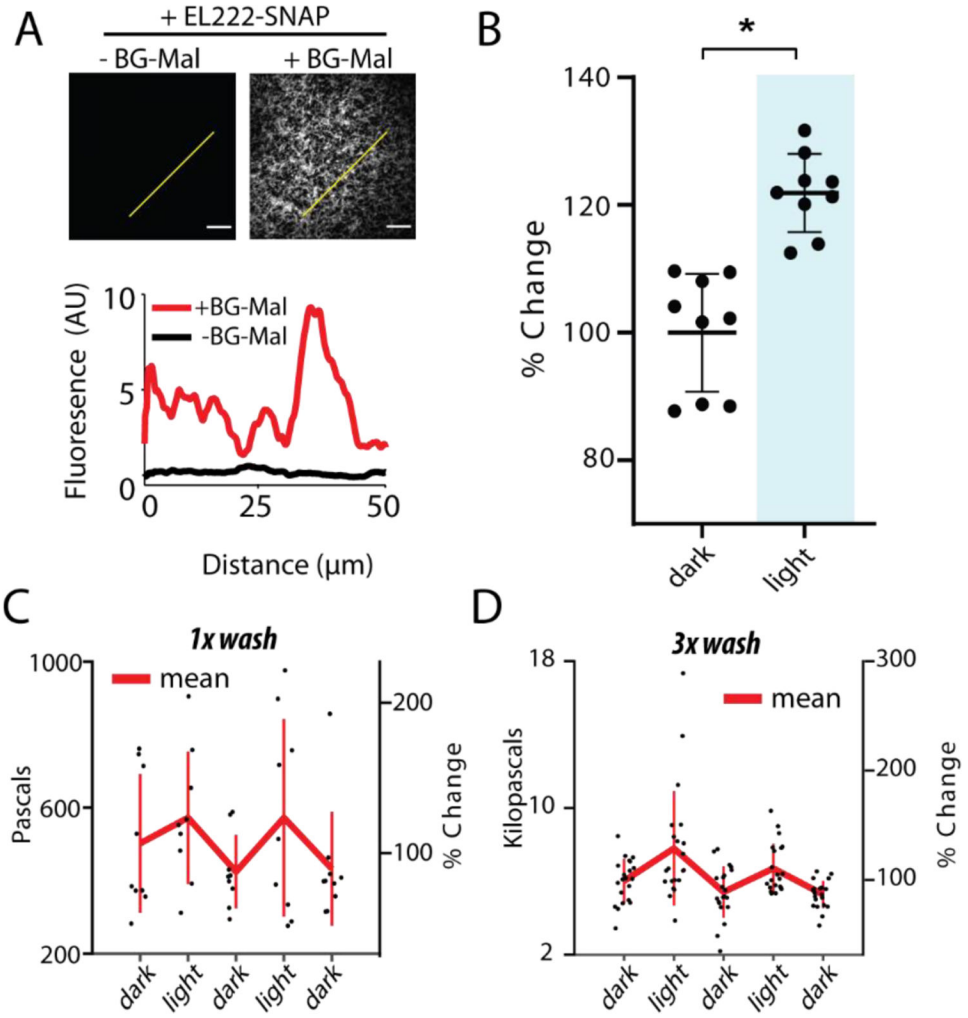

Figure 3. EL222-SNAP Binds and Alters Mechanical Properties of Collagen Hydrogel.

A) (*Top*) 1 mg/mL collagen hydrogel functionalized with EL222-SNAP with (*right*) and without (*left*) a prior BG-Mal incubation. mCherry signal, from EL222-SNAP, is shown. Scale bar = 10 μm. (*Bottom*) Fluorescence intensity across 50 μm trace (yellow line) of above images. B) Percent change of elastic modulus, as determined by IT-AFM, of EL222 OptoGels during activation. * represents $p < 0.05$. C) Elastic moduli of EL222 OptoGel during 2 sequential activations. D) Elastic moduli of EL222 OptoGel made with 3 EL222-SNAP incubations (versus 1) during 2 sequential activations. Absolute averages for 3C and 3D reported in Table S2. Percent change is calculated from the mean.